
Design optimization and control of a double stator permanent magnet generator for tidal energy applications

Jian Zhang, Luc Moreau, Azeddine Houari, Mohamed Machmoum

*IREENA, Université de Nantes
37 Bd de l'Université BP. 406
44602 Saint-Nazaire CEDEX
mohamed.machmoum@univ-nantes.fr*

***ABSTRACT.** This paper investigates a variable speed direct drive optimization and control for marine current energy application based on a Double Stator Permanent Magnet Generator (DSPMG). At first, turbine concepts, relative projects and usual conversion chains for tidal energy conversion are briefly presented. An original generator multi-objective optimal design method taking into account the tidal speed occurrence, control strategy and converter size to minimize the investment and maximize the annual energy output is developed. The conceptual advantages of the DSPMG are also used to show the possibility of uninterrupted operation under converter open phase faults. Simulation results are given and demonstrate the effectiveness of the optimization design and the proposed fault tolerant control.*

***RÉSUMÉ.** Ce papier traite de la commande et de l'optimisation d'une génératrice synchrone à aimants permanents à double stator (DSPMG) pour une application de l'extraction de l'énergie des courants marins. Dans un premier temps, nous présentons différents concepts de turbines et les projets en cours. Nous avons développé une optimisation originale de dimensionnement de l'ensemble convertisseur machine qui tient compte à la fois des probabilités d'apparition de vitesse de courants marins, de la stratégie de commande, du design du générateur ainsi que de la taille du convertisseur de façon à minimiser l'investissement et maximiser l'énergie annuelle produite. Ensuite, nous mettrons en évidence que les avantages structurels intrinsèques de la DSPMG permettent de fonctionner en régime dégradé avec une phase en défaut, tout en assurant la continuité de service. Enfin, les stratégies de contrôle développées en régime dégradé sont présentées et analysées.*

KEYWORDS: marine current renewable energy, modelling, optimal design, double stator permanent magnet machine, fault-tolerant control.

MOTS-CLÉS : énergie hydrolienne, modélisation, design optimal, génératrice synchrone à aimants permanents à double stator, commande en mode dégradé.

DOI:10.3166/EJEE.18.339-359 © Lavoisier 2016

1. Introduction

To provide a sustainable power production in the future and respecting the Kyoto protocol at the same time, there is a growing demand for energy from renewable sources such as wind, geothermal, solar and ocean. A leading sector is the ocean renewable energy. Indeed, the oceans cover more than 70% of the earth's and can produce much more energy than other sources every year (Chen *et al.*, 2016). According to authority, global ocean resource is estimated between 2,000 and 4,000 TWh per year.

The most prominent and studied techniques of exploiting and extracting ocean energy are classified as follows: wave energy, tidal energy, osmotic energy, ocean thermal energy and cultivation of the marine biomass (S. E. Benelghali *et al.*, 2007). However, marine current energy has the remarkable advantage of highly predictability which makes it more attractive than the other renewable energy (Anwar *et al.*, 2017; Fox *et al.*, 2017).

France has a huge potential for exploiting marine current renewable energy, coupled with strong R&D and industrial capabilities to develop these technologies for the market (Campbell *et al.*, 2017). To achieve this goal, French government sectors, laboratories and companies collaborate to build a complete research and development of systems including funding, source modelling, experiment, generator design, converters, transmission, and integration to the grid.

Our laboratory IREENA is currently carrying an interregional project called Hydrol 44 involving academic and industrials partners whose purpose is to organize a "task force" in the West region of France dedicated to the study of marine current energy conversion systems. This work is realized in this context and the paper will be organized as follows. Section 2 describes the advantages, technological challenges and usual conversion chains of marine current energy. An example of typical marine current energy conversion chain based on a Double Stator Permanent Magnet Generator (DSPMG) is detailed in section 3. An original generator optimal design method taking into account the tidal speed occurrence, control strategy and converter size to minimize the investment and maximize the annual energy output is developed in section 4. Section 5 investigates the open circuit fault tolerant performances of a DSPMG in tidal power generation system. Conclusions are presented in section 6.

2. Marine current energy

2.1. Principle, advantages and, challenges

As a renewable resource, marine current energy has the distinct advantage of being predictable compared with other forms of renewable energy, up to 98% accuracy for decades, which make the marine current energy development an attractive resource option. It is mainly independent of prevailing weather conditions that can highly impact other renewable generation forecasts.

Besides, another important characteristic is the high power density caused by sea density (800 times larger than air density), as the kinetic power varies depending on the density and the cube of velocity of the marine current, the marine current speeds are almost one-tenth the speed of wind for the same power. So, the size and the weight of a marine current turbine can be much smaller than the similar rated power of wind turbine (one-tenth, one twentieth respectively).

The basic physical principles for extracting energy from marine currents are virtually identical to those of wind energy. Many researchers suggest using the similar techniques which has been successfully developed for Wind Energy Conversion System (WECS). However, there are numerous differences and difficulties in the design of Marine Current Turbine (MCT), including stall characteristics and the possible occurrence of cavitation in the blades. A special attention is that the MCT has shorter and thicker blades than Wind Turbine in order to withstand the larger stresses due to the higher density of the water.

However, regardless of turbine design, only a fraction of hydrodynamic power in the free marine current is recoverable. The power coefficient C_p , which is also called Betz's coefficient, allows describing the ratio of recoverable power. Then, the extractable mechanical power P_m of MCT is expressed by the following relation:

$$P_m = \frac{1}{2} C_p \rho A V_{tide}^3 \quad (1)$$

The power coefficient C_p is obtained based on Blade Element Momentum (BEM) theory. It highly depends on the TSR (Tip Speed Ratio or λ), the pitch angle β , the number and the geometry of the blades. For WECS, C_p has typical values in the range 0.25~0.5. However, for MCECS, this value is estimated to be in the range 0.35~0.5.

MCT devices can be classified in a number of different ways with overlap between categories. In this paper, these devices will be classified depending on the way they interact with the water in terms of motion. So, the whole of the different models available could be mainly classified as follows (Zhang, 2015):

- Horizontal Axis Turbines;
- Vertical Axis Turbines;
- Oscillating Hydroplane Systems.

Nowadays, the majority of the marine current devices are the horizontal axis turbines. Depending on turbine design, their blades can either have a fixed pitch or variable pitch to enable the turbine to operate during flow in both directions (Rourke *et al.*, 2010). On the other hand, based on the experience of tested prototypes and commercial projects, some common technological challenges become more and more thorny. The most pressing problems on which all researchers must confront at present are installation, maintenance, packing density and fouling phenomena.

2.2. Horizontal axis turbines and usual generators

There are many projects and concepts proposed and tested for horizontal axis system. The existing marine current systems can also be divided into two kinds: Geared Drive Train System including Induction Generators (IG) and Permanent Magnet synchronous generator (PMSG), and Direct Drive Train System based principally on synchronous generators.

The world's first grid connected commercial project - Seagen S (UK, 1.2MW at $2.4m/s$, installed in Strangford in May 2008 and owned by Siemens since 2012) and 1MW precommercial project - HS1000 (see Figure 1 (MCT.Ltd, 2012) and Figure 2 (Andritz-Hydro-Hammerfest, 2014)) preferred to use induction generator. This Seagen device comprises twin axial flow rotors of 16m diameter, each driving an induction generator through a gearbox. These twin turbines can be operated independently. The rotors have a patented full span pitch control which allows them to operate on both flood and ebb tides. These two rotors can be raised above the surface for safe and easy maintenance access. The Seagen has already generated 8GWh electricity since the installation.



Figure 1. Seagen turbine



Figure 2. HS1000



Figure 3. 1 MW turbine for Alstom/GE



Figure 4. Open-Centre Turbine

In 2013, Alstom completed the acquisition of Bristol-based Tidal Generation Ltd (TGL), which was established in 2005. In September 2010, TGL developed a 500kW tidal stream turbine based on a classical induction generator - Deepgen - which was successfully deployed and connected to the grid at EMEC's tidal test site at the Fall of Warness in Eday (see Figure 3 (Alstom, 2013)). In March 2012, TGL announced that the device had generated over 200MWh into the national grid since installing their device on site. In 2014, Alstom has been chosen by EDF to equip 4 Oceade TM 18 (1.4MW) turbines at Raz Blanchard tidal pilot farm.

Until now, based on literature, only Uldolmok (the strait of the strongest tidal current in Korea, located at the southwestern tip of the Korean Peninsula) pilot tidal current power plant of 1MW would use DFIG.

A lot of other projects choose PMSG structure such as: Gorlov Helical Turbine and EnCurrent Turbine, even for some larger scale like AR1000. AR1500, 1.5MW, is a pitchable, gearbox integrated and permanent magnet generator. It is developed by a Canada tidal power generation company - Atlantis Resources Corporation (Atlantis, 2015).

PMSG has already been proved to be the most attractive choice for a direct driven WECS as its highest yield energy, higher robustness, reliability and power to weight ratio although more expensive price (Li, Chen, 2008; S. Benelghali *et al.*, 2012). In a direct drive train system, the generators are directly driven by the turbine hub or the turbine blades. It means the generator will rotate at a very low nominal speed in

the range of $5 \sim 50 \text{ rpm}$ depending on the turbine size, the current velocity and the site condition. In comparison with conventional high speed generators, they have a much larger diameter for implementation of a large number of poles, almost the same efficiency and about the same total weight, but a slightly higher price presently. The direct drive generators always have a very high rated torque which is a significant difference between the low and high speed machines as the size and the losses of a low-speed generator depend on the rated torque rather than on the rated power.

Open-Centre Turbine (also called rim driven generator system) has a high solidity horizontal axis rotor with symmetric, fixed pitch blades. The alignment of the rotor to the flow is fixed. Power generation is accomplished by a variable speed circumferential Direct Drive PMSG incorporated into the enclosing shroud. The center section of the rotor is open. The turbine is secured to the seabed by a tripod gravity base. Figure 4 gives one 2MW rated power tidal turbines which is tested in the Bay of Douarnenez on 2011 (Openhydro, 2014). This project is cooperated between EDF and Open Hydro, and aims to deploy four 2MW MCECS for the first marine current park in France.

IREENA laboratory (ST Nazaire, France) is currently carrying an inter-regional project called Hydrol 44 whose purpose is to organize a "task force" in the West region dedicated to the study of marine current energy conversion chains. The researches carried-out in the laboratory IREENA are focused on special Direct Drive PMSG design and fault tolerant control, such as Doubly Salient Permanent Magnet Generator, five phase permanent magnet generator and Double Stator Cup Rotor Permanent Magnet Generator (DSPMG) (Chen *et al.*, 2016; Dieng *et al.*, 2014; Zhang, 2015). On the following, some developments will be detailed concerning optimisation design and control of a conversion chain based on a DSPMG.

3. Modelling of DSPMG conversion chain

3.1. Energy conversion chain

The studied system is shown by Figure 5. It is composed of fixed pitch direct drive turbine, DSPMG, converters and the grid. The two stators are separately connected to the DC-bus through two voltage source converters. The generator side and the grid side converters are separately controlled. The rated generator power is 1MW and the rated speed is 21.5 rpm .

Figure 6 shows the structure of the DSPMG. The permanent magnets are surface mounted on the two sides of the cup shape rotor. In order to reduce the cogging torque, the magnets are shifted one slot degree. There are two air gaps in the machine. Through increasing the air gap surface comparing conventional single stator machine, the machine torque volume density is increased. Tidal current turbine is much smaller than wind turbine for the same power rate as the water density is more than 800 times of the air density. High torque volume density characteristic makes DSPMG really suitable for tidal current energy application.

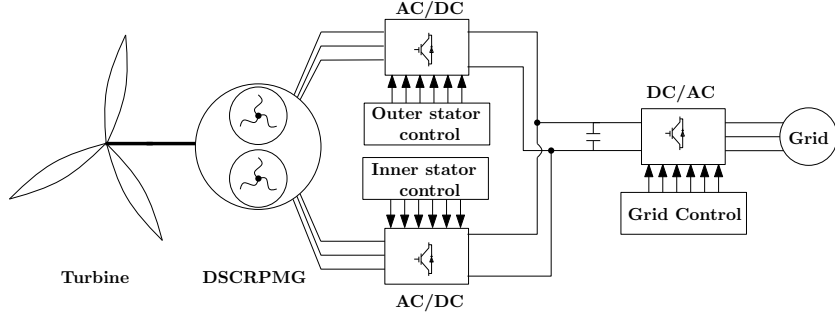


Figure 5. System description

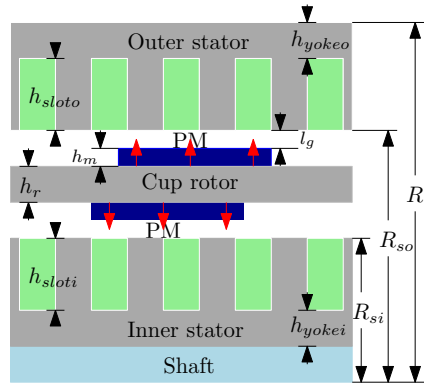


Figure 6. Generator structure

3.2. Design model

The machine design is based on fundamental flux density harmonic. The rated power is 1MW. Rated phase to phase voltage is 690V. Rated speed is 21.5rpm. The external machine radius is 1.5 meter which is chosen based on commercial MW range PMSM.

In the following, the subscript k is used to represent the outer stator (o) or inner stator (i). Both outer stator and inner stator have similar model equations. On the following the principle phases of analytical model are summarized:

The EMF is given by the following equation:

$$E_k = \frac{1}{\sqrt{2}} \omega_e k_{wk} N_k \psi_k \quad (2)$$

where N_k is the number of turns per phase and ω_e is the electrical rotational speed with: $\omega_e = p\omega_m$ (where ω_m is the mechanical rotational speed and p is the number of pole pair). k_{wk} is the winding factor and ψ_k is the peak fundamental flux in air gap.

The inductance is one of the most important information that generator designers should provide it to control designers. The direct-axis synchronous inductance L_{dk} consists of the direct-axis magnetizing inductance L_{mdk} and the leakage inductance $L_{s\delta k}$:

$$L_{dk} = L_{mdk} + L_{s\delta k} \quad (3)$$

The direct-axis magnetizing inductance L_{mdk} for multiphase machine includes not only the phase self-inductance part, but also the inductance caused by the other phases. For m phases machine, the magnetizing inductance is equal to product of $m/2$ and the phase self-inductance. The second part of d-axis inductance is the leakage inductance $L_{s\delta k}$. Both magnetizing inductance L_{mdk} and leakage inductance $L_{s\delta k}$ calculations are detailed in (Pyrhönen *et al.*, 2014).

The total copper losses in the stator k are:

$$P_{cuk} = \frac{3}{2} I_{sk}^2 R_{cuk} \quad (4)$$

I_{sk} is the amplitude of phase current. R_{cuk} is the phase resistance which is calculated from the machine parameters.

For the iron losses, the principle of separation of losses is applied, including both hysteresis losses and eddy current losses. The total iron losses are the sum of yoke iron loss $P_{ironyokek}$ and teeth iron loss $P_{ironteethk}$:

$$\begin{aligned} P_{ironk} &= P_{ironyokek} + P_{ironteethk} \\ &= (k_{ec} f^2 + k_h f) (B_{yokek}^2 M_{yokek} + B_{teethk}^2 M_{teethk}) \end{aligned} \quad (5)$$

where f is the operation electrical frequency. k_{ec} and k_h are the specific loss coefficients for eddy currents and hysteresis, respectively. Their value can be approximately estimated from the data sheet of core material. M_{yokek} and M_{teethk} represent the iron mass of the yoke and teeth respectively. The maximum flux density in yoke and teeth, B_{yokek} and B_{teethk} , can be calculated from maximum air gap flux density (Zhang, 2015).

For the generator thermal modeling, the temperature of the winding T_{cuk} is the sum of temperature rising in conductor $\Delta\theta_{cuk}$, stator iron $\Delta\theta_{ironk}$ and ambient temperature T_A . For tidal energy application, $T_A = 20^\circ C$ is taken because the generator is operated under the sea water.

$$T_{cuk} = \Delta\theta_{cuk} + \Delta\theta_{ironk} + T_A \quad (6)$$

$\Delta\theta_{cuk}$ and $\Delta\theta_{ironk}$ are calculated from the generator power losses, heat transfer coefficient and heat transfer surface (Zhang, 2015).

3.3. Machine model for control

The mathematical model of double stator generator in view of control can be simply written as the combination of two conventional single stator PMSG models expressed in dq reference frame.

$$\begin{bmatrix} v_{dk} \\ v_{qk} \end{bmatrix} = R_{cuk} \begin{bmatrix} i_{dk} \\ i_{qk} \end{bmatrix} + \begin{bmatrix} L_{dk} \frac{d}{dt} & -L_{qk}\omega_e \\ L_{dk}\omega_e & L_{qk} \frac{d}{dt} \end{bmatrix} \begin{bmatrix} i_{dk} \\ i_{qk} \end{bmatrix} + \begin{bmatrix} 0 \\ \omega_e \psi_k \end{bmatrix} \quad (7)$$

For surface mounted permanent magnet machine, $L_{dk} = L_{qk}$. The total electromagnetic torque is

$$T_e = T_{eo} + T_{ei} = \frac{3}{2} p \psi_o i_{qo} + \frac{3}{2} p \psi_i i_{qi} \quad (8)$$

The most common control method is Maximum Torque Per Ampere control (MTPA) which keeps the d axis current equal to zero. However, this control strategy can only minimize the copper losses. In this paper, the d axis current is controlled in a manner of minimizing system losses (copper, iron and converter total losses). The q axis current is controlled to provide the needed load torque.

The modeling of the DSPMG is completed by the mechanical equation given by:

$$T_e = T_L - J \frac{d\omega_m}{dt} - f_v \omega_m \quad (9)$$

where J is the rotor inertia, T_L is the turbine torque and f_v is the viscous damping.

4. DSPMG multi-objectives optimization

Every machine optimization problem is defined by: objective function(s), a set of variables, and constraints. For a randomly set of variable values, the objective functions can be calculated. By comparing the objective values (minimum or maximum) found for different sets of variables, an optimal set of variables is reached. The calculation process should satisfy the constraints imposed by mechanical, magnetic and electronic phenomenon in machine optimization process.

4.1. Objectifs functions

– F_{obj1} -Maximize annual energy output:

The power harnessed by turbine will be transferred to the electrical conversion chain through the shaft connection. The mechanical losses are neglected in our optimization model. The produced electrical power for operating point can be expressed as:

$$P_{elec,j} = T_j \omega_{m,j} - P_{cu,j} - P_{iron,j} - P_{conv,j} \quad (10)$$

Where P_{conv} is the converter losses and it is calculated from conducting losses and switching losses of the electrical device (Aubry *et al.*, 2012). Then, the output energy in one year can be expressed by the following equation:

$$F_{Obj1} : \quad E_{elec} = \sum_{j=1}^{N_{pts}} P_{elec,j} t_j \quad (11)$$

N_{pts} is the machine operating point number. The predicted tidal current speed is separated into N_{pts} points. For each speed, there is corresponding optimal machine torque and speed.

– F_{Obj2} : Minimize machine and converter cost:

The second optimization objective is to minimize the total electrical conversion chain investment. The generator raw material $C_{generator}$, generator structure $C_{structure}$ and converter cost C_{conv} are considered in the design model. Therefore, the system cost can be expressed as follow:

$$F_{Obj2} : \quad C_{system} = C_{generator} + C_{structure} + C_{conv,k} \quad (12)$$

The material cost of generator is estimated from the weight of active parts including copper, iron and permanent magnet. The machine supporting structure is required to maintain the airgap clearance (McDonald *et al.*, 2008). Its cost can be approximately calculated by machine length and diameter (Grauers, 1996). For the cost of converter, it is based on the apparent rated power (Aubry *et al.*, 2012).

4.2. Variables and constraints

The design of the generator is based on analytical model. The geometries are design variables (see Figure 6). The machine external radius R is fixed as 1.5m. Then There are totally 16 parameters to be optimized including machine external shape parameter such as outer stator power percentage k_1 , pole pairs p , machine length L , bore radius R_{so} and the used converter apparent power $S_{conv,k}$. It also includes machine inner geometry parameters such as air gap l_g and magnet thickness h_m , yoke thickness h_{yoke} and slot height h_{slot} . The conductor number N_{slotk} in one slot is also optimized. Their optimal design range are shown in the Table 1.

The Constraints or technological limits are:

- Total cost constraint: $C_{system} \leq 1M\text{€}$
- Geometry constraints: $R_{so} + h_{yoke} + h_{slot} < R$, $R_{so} - h_r - 2(l_g + h_m) - h_{yoke} - h_{slot} > 0$, $l_g \geq \frac{2R_{so}}{500}$
- Magnetic saturation constraints: $B_{x,j} < B_{sat}$, where x represent different parts of the generator (the outer and inner stator teeth, yoke, cup shape rotor).
- Demagnetization: $H_j < H_c$. H_c is the intrinsic coercivity field.
- Electrical constraints: $V_j < V_{max}$; $I_j < I_{max}$. The generator voltage and current should be smaller than the maximum capability.
- Winding temperature constraint: $T_{cuk}, j < 155^\circ\text{C}$.

Table 1. Optimization parameters.

Symbol	Description	Region	Unit
k_1	Power percentage of outer stator	[0.5;0.7]	-
p	Pole pairs	[2;200]	-
k_t	Tooth width/slot pitch	[0.2;0.8]	-
R_{so}	Outer stator bore radius	[0.5;1.5]	m
h_{yokeo}	Thickness of outer stator yoke	[0.1;50]	cm
h_{sloto}	Height of outer stator slot	[0.1;50]	cm
l_g	Airgap length	[1;10]	mm
h_m	Thickness of magnet	[1;50]	mm
h_r	Thickness of cup rotor	[0.1;100]	cm
h_{yokei}	Thickness of inner stator yoke	[0.1;50]	cm
h_{sloti}	Height of inner stator slot	[0.1;50]	cm
L	Active machine length	[0.01;5]	m
N_{sloto}	Conductor number in one outer slot	[1;30]	-
N_{sloti}	Conductor number in one inner slot	[1;30]	-
S_{conv0}	Outer stator converter apparent power	[0.01;5]	MVA
S_{conv1}	Inner stator converter apparent power	[0.01;5]	MVA

4.3. Optimization process

Figure 7 shows the flow chart of the multi-objectives optimization design process. Firstly, the machine geometries and converter apparent power are randomly generated in the region of their corresponding upper and lower boundary. If the randomly generated variable parameters do not satisfy the geometry constraints, the optimization algorithm will then regenerate another set value of the variables. Once the parameters satisfy the geometry constraints, the machine parameters can be calculated such as inductance, flux, mass.... From the generator active mass and converter apparent power, the cost of the system can be calculated. For each operating point j , the currents can be decided according to the needed torque. Then, the electrical, magnetic and thermal constraints are verified. If not all the operation points satisfy the constraints, the optimization algorithm will generate another set of machine and converter parameters once again. The algorithm will stop when it reaches a predefined iteration criteria.

4.4. Results

In following pareto front figures, the red point and magenta point refer to the design solutions which can maximum 20 years revenue and minimum cost energy ratio respectively.

Figure 8 shows the Pareto front results and four extreme solution are indicated. Every point in the Pareto front is one set of machine converter system parameter or called candidate design solution. This figure illustrates that the candidate design solution is a trade-off between the energy output (income) and the initial cost (investment). In

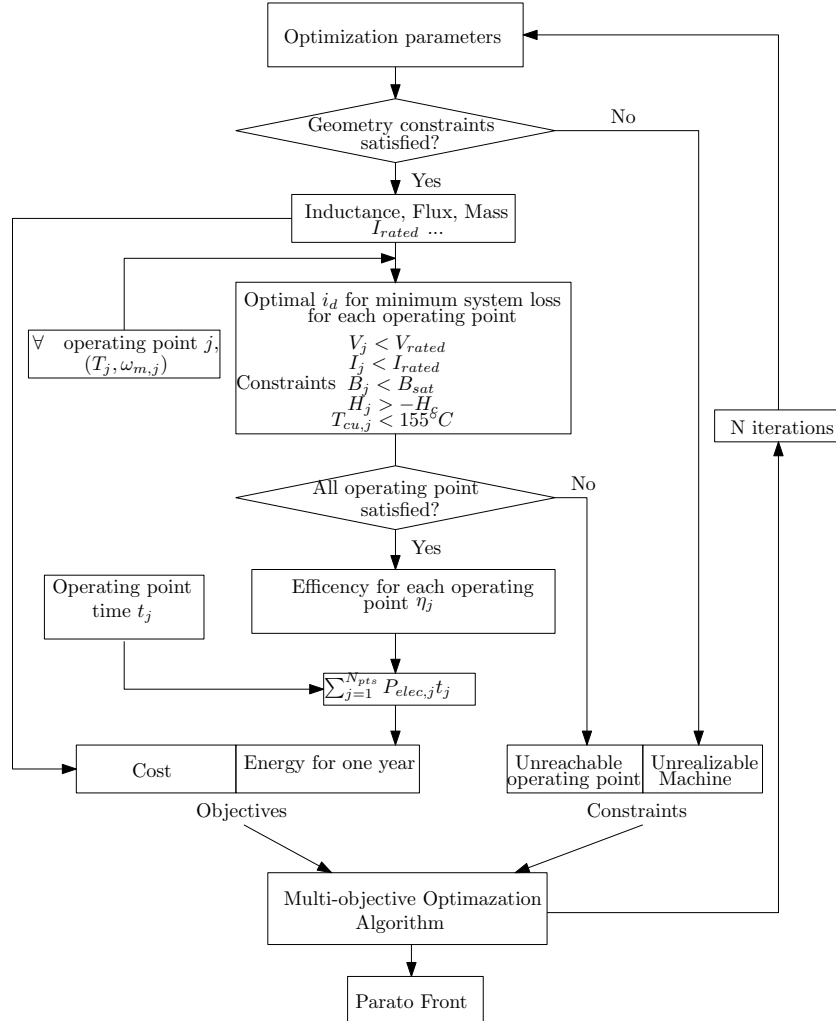


Figure 7. Optimization flow chart

the low energy output region, the total initial cost is also relatively low and vice versa. The annual energy output can be increased a lot without increasing too much of initial cost in the low energy region. However, in the high energy output region, the total initial cost increases much quicker than the annual energy output. It is clearly shown that one can't improve one objective without degrading the other one from the Pareto front figure. All potential design solution in pareto front are optimal solution. The final design solution depends on the customer selection criteria. Some important parameters for four special generator design solutions in the Pareto front are indicated in Table 2.

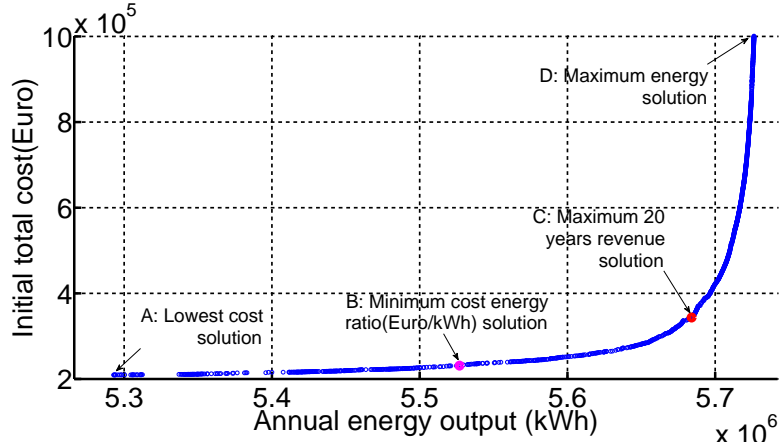
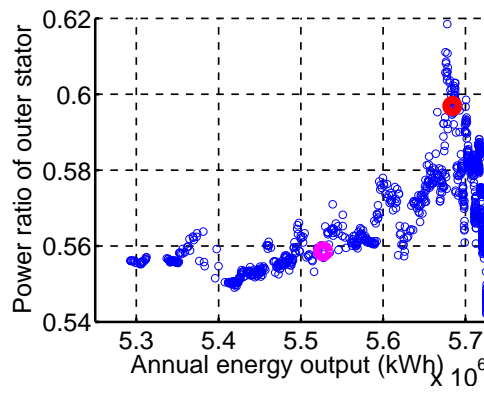


Figure 8. Pareto front of the optimization results

Table 2. Key parameters of the four special design solutions.

Symbol	A	B	C	D
$E_{elec}(M.kWh)$	5.29	5.53	5.68	5.73
$C_{system}(k\text{\euro})$	209.5	231.2	344.6	1000
p	54	44	22	12
$R_{so}(m)$	1.415	1.390	1.251	1.150
$L(m)$	0.517	0.626	1.040	2.307
$h_{yokeo}(mm)$	17	20	36.8	73.5
$h_{sloto}(mm)$	63.5	86	208.4	272
$h_r(mm)$	31	38	65	82
$S_{conv}(MVA)$	0.6	0.62	0.67	2.96
$T/M(N.m/kg)$	62.9	39.3	12.2	4.24
$T/V(kN.m/m^3)$	121.6	100.5	60.4	27.2

Figure 9. Profile of optimization parameter outer stator power ratio k_1 vs. the first objective.

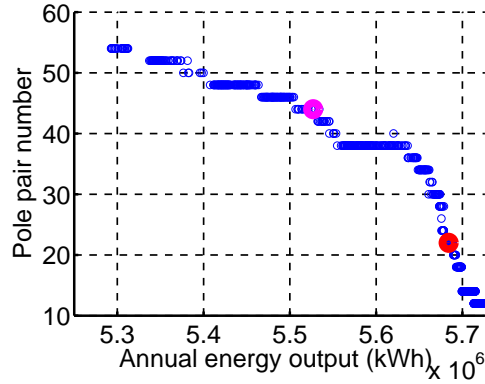


Figure 10. Profile of optimization parameter pole pairs number p vs. the first objective.

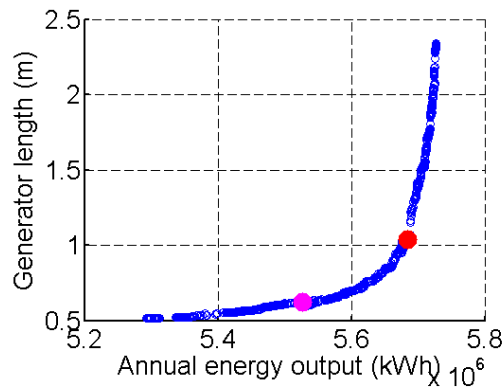


Figure 11. Profile of optimization parameter machine length L vs. the first objective.

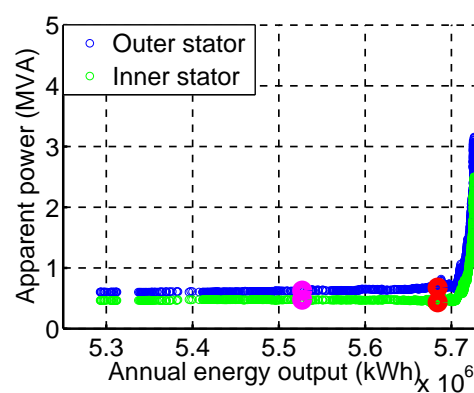


Figure 12. Profile of optimization parameter stator converter apparent power S_{conv} vs. the first objective.

Figure 9, Figure 10, Figure 11 and Figure 12 present the evolution of some optimization parameters varying with the objective function. The outer stator power percentage k_1 varies between 0.54 and 0.61 which confirms that it is reasonable to design a double stator machine with bigger rated power for outer stator than that of inner stator.

As the nominal torque is fixed by the turbine, and the machine torque varying with $p^2 L$, pole pair number evolution has inverse trends with the machine length L . The converter apparent powers are almost constant in the majority energy range for inner and outer stator as shown in Figure 12. In the high energy high cost region, the algorithm tends to search the possible solution to increase the annual energy output and the converter sizes will unavoidable increased.

5. Control of a DSPMG conversion chain

In the control part, the minimum cost energy ratio solution (point B in Figure 8) is used to design the control system. Regarding the machine conception, the total torque is resulted from the superposition of the two stator torques. This paragraph proposes to analyze system performances under healthy conditions or under converter open phase fault.

5.1. Healty conditions

Figure 13 illustrates the control system of the DSPMG. Generator rotational speed is controlled to the needed reference value (normally to realize maximum power point tracking or flux weakening control). Each stator has its own inner dq axis current control loop. Five PI controllers are then used: speed controller, outer stator I_{do} and I_{qo} current controllers and inner stator I_{di} and I_{qi} current controllers. The d axis reference currents of inner and outer stator are fixed as zero to achieve maximum torque per ampere control. As the total electromagnetic torque is produced by the sum of the two stators, q axis reference currents are obtained by multiplying the output of speed PI controller by power percentages k_1 and k_2 for outer and inner stator respectively. The power percentages k_1 and k_2 are obtained in the machine design process. k_1 is bigger than k_2 . The current loop controllers of outer and inner stator are tuned with Optimal Modulus (OM) criterion and the speed loop controller is tuned with Optimum Symmetric Method (OSM) (Panda, 2012; Mehrzad *et al.*, 2009).

5.2. Fault tolerant control

It is assumed that the open circuit fault happened in outer stator phase a ($i_a = 0$). Open circuit fault is a common default in industry machine drive system which may be caused by converter abnormal function. Short-circuit, by mean of fast fuse, also

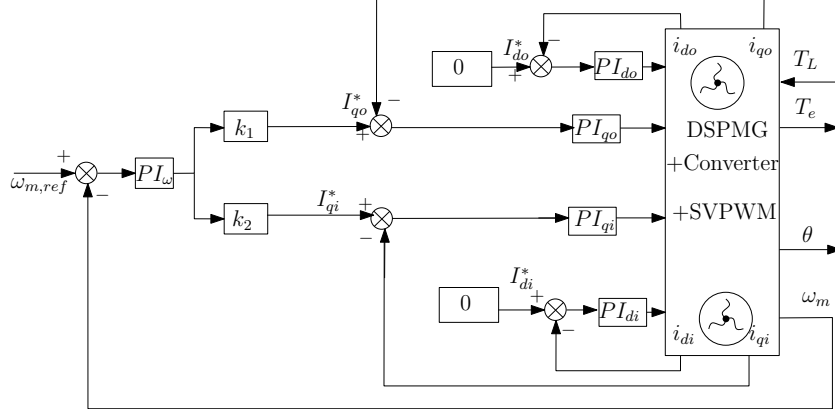


Figure 13. Generator control scheme

leads to open circuit fault. The machine dq axis currents will start oscillating with a doubled frequency as the following equation indicates (Zhang *et al.*, 2016):

$$\begin{bmatrix} i_{do} \\ i_{qo} \end{bmatrix} = \mathbf{T}_{abc \rightarrow dq} \begin{bmatrix} i_a \\ i_b \\ i_c \end{bmatrix} = \frac{\sqrt{3}}{3} I_{mo} \begin{bmatrix} \sin(2\theta) \\ 1 + \cos(2\theta) \end{bmatrix} \quad (13)$$

where $\mathbf{T}_{abc \rightarrow dq}$ is the Park transformation matrix.

The outer stator torque will also oscillate as the q axis current. The average torque of the faulty stator will decrease to 58% of the torque in health condition for the same current amplitude.

$$\frac{T_{eo_{fault}}}{T_{eo_{health}}} = \frac{\frac{3}{2}p\psi_{mo} \frac{\sqrt{3}}{3} I_m}{\frac{3}{2}p\psi_{mo} I_m} = \frac{\sqrt{3}}{3} \approx 0.58 \quad (14)$$

In order to obtain continuity service of system, a fault tolerant control method is proposed. The proposed approach is fulfilled in two steps. First, modifying the faulty stator dq axis currents to force the remaining healthy phase currents in opposite. The second step uses high pass filter based compensator to cancel the undesirable faulty stator torque ripple by modifying the healthy stator current reference. The modified control structure is shown in Figure 14 and the two steps are indicated as block 1 and 2. The high pass filter based compensator in block 2 superposes an appropriate compensating signal in the q -axis current loop of the healthy stator so that the modified control rejects the torque ripples caused by the faulty stator. The injected compensating current $i_{qo,comp}$ to the inner stator (healthy stator) q -axis current reference can be expressed as:

$$i_{qo,comp} = \frac{s}{s + 2\pi f_c} K_c i_{qo} \quad (15)$$

where K_c is the compensating gain whose value is set to 0.8. The filter cutoff frequency f_c is set to be sufficiently smaller than the torque oscillating frequency at the rated operation. Hence, f_c is fixed to 5 Hz.

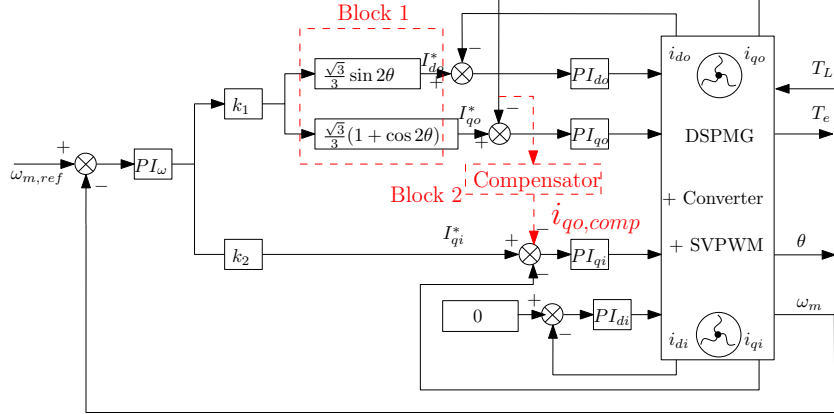


Figure 14. Proposed fault control diagram

5.3. Results

Simulations have been carried out using MATLAB/Simulink. The fault comes out at rated operating condition ($T_e = 0.44MN.m$ and $N = 21.5rpm$).

Figure 15 and Figure 16 show the behavior of the measured states, respectively the speed and electromagnetic torque without and with the proposed compensator.

The open phase fault is applied at $t = 0.5s$. Before $t = 0.5s$, the DSPMG system operates in healthy condition. The speed and torque follow their references. When open phase fault occurs at $0.5s$, it can be observed that the speed oscillation is around 3.7% when without compensator. This oscillation is significantly reduced with the use of the proposed compensator shown in Figure 16. Also, it can be noted that the peak-to-peak electromagnetic torque ripples are minimized with the use of the compensating method. At open phase condition, the outer stator capability is reduced; the inner stator increases its produced torque to compensate the torque which outer stator can't produce. They have inverse variation form.

Figure 17 and Figure 18 show that the two stator current forms for the control condition without and with the proposed compensator. One phase current of the outer stator becomes zero when the open circuit fault happen (phase A). The other two phase currents are in opposite. The phase current amplitude of the inner stator are increased for compensating the torque decreasing of the outer stator which has open circuit fault in both cases with or without using compensator. The relative phase current of the healthy stator increases bigger than the other phases: when phase A of outer stator is open, the phase A of inner stator increase bigger than the other two. The inner stator currents become unbalanced.

It can be envisaged that the efficiency of the system in fault condition is decreased because of the increasing of currents. The generator thermal issues and overloaded margin should be carefully investigated in the machine design process. That may lead

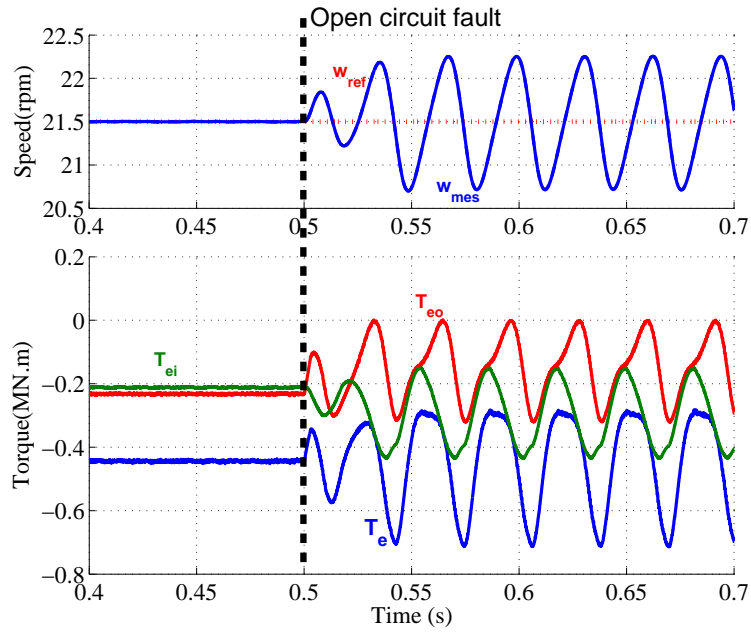


Figure 15. Torque and speed response without the proposed compensator

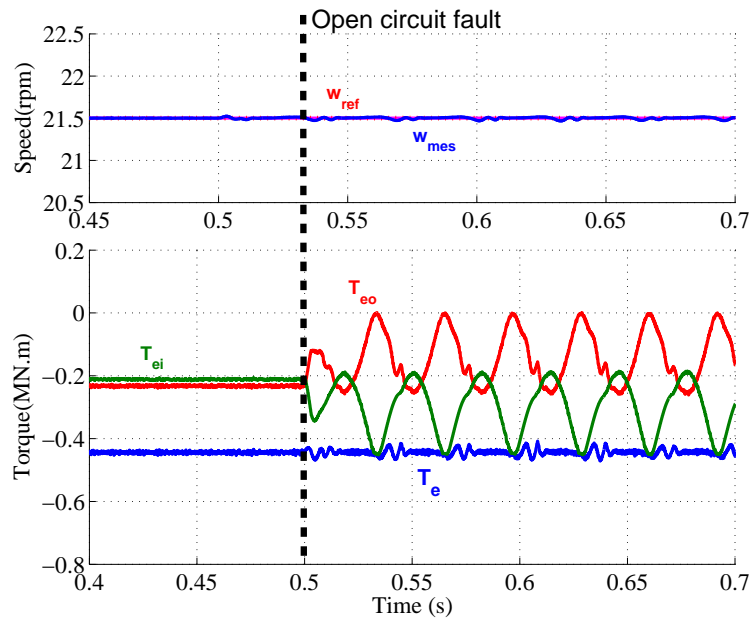


Figure 16. Torque and speed response with the proposed compensator

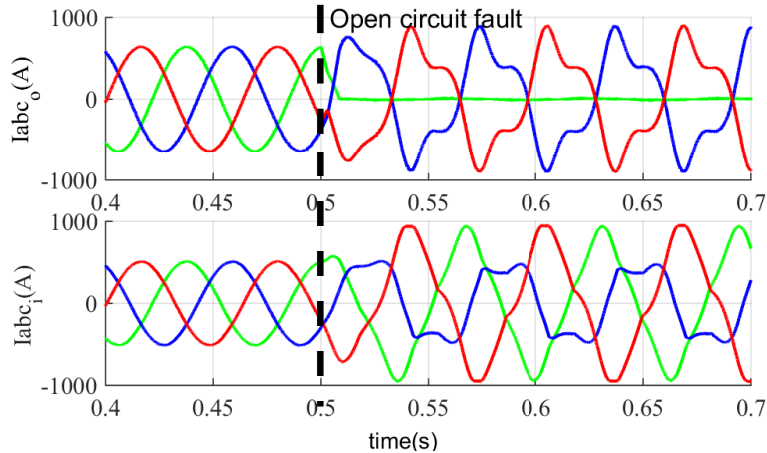


Figure 17. Behavior of the stator currents without the proposed compensator

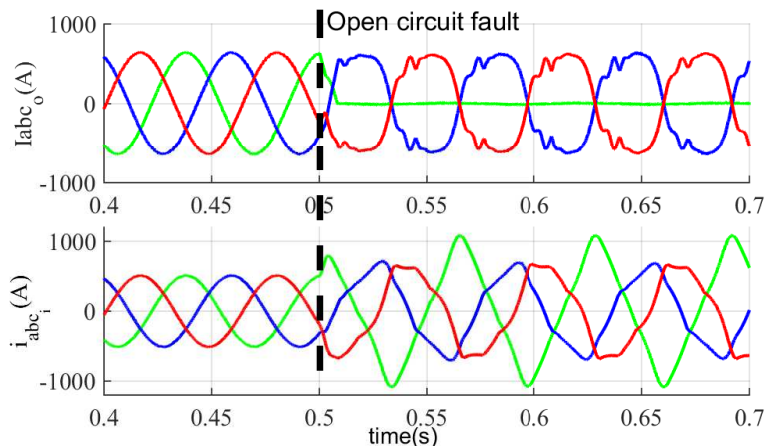


Figure 18. Behavior of the stator currents with the proposed compensator

higher machine design investment. It can be seen from the stator currents that the fault condition control with compensator has less serious thermal problem. In the case of serious fault condition, like 2 open phases, the faulty stator can be totally shunted down and only keeping the health stator transfer the turbine energy to the grid. If the thermal limit margin is large, the health stator can be operated to compensate the shunt down stator power. Otherwise, the input shaft power should be reduced to the health stator power level. The results show that this machine can provide the possibility of high continuity of service in the case of open phase fault.

6. Conclusion

This paper has presented a brief review of marine current energy. Different projects are classified according to their technology challenges, turbine concepts and used generator/converter interfaces. This synthesis shows that direct drive systems seems the best choice for marine current energy conversion systems.

A typical conversion chain based on a doubly stator permanent magnet generator is then studied. An original approach minimizing both losses of the machine and the converter is proposed, leading to improve the system efficiency over the whole speed range (MPPT and flux weakening regions). A multi-objective optimization of investment and energy extracted by the entire conversion chain is performed for an operating period of 20 years, taking into account the occurrence of sea current speed probabilities.

Finally the behavior of the conversion chain under converter open phase fault is analyzed. A fault tolerant control is proposed to achieve a smooth torque, equals to the one under normal conditions, and reject undesirable torque ripples. The provided simulation results demonstrated that DSPMG offers a degree of freedom for achieving reliable operation in marine power generation.

References

- Alstom. (2013). <http://scotsrenewables.com/blog/tidalpower/alstoms-tidal-turbine-reaches-1mw-in-offshore-conditions/>. ([Online; accessed 19-September-2018])
- Andritz-Hydro-Hammerfest. (2014). <http://www.andritzhydrohammerfest.co.uk/>. ([Online; accessed 19-September-2018])
- Anwar M. B., Moursi M. S. E., Xiao W. (2017, March). Novel power smoothing and generation scheduling strategies for a hybrid wind and marine current turbine system. *IEEE Transactions on Power Systems*, Vol. 32, No. 2, pp. 1315-1326.
- Atlantis. (2015). <http://atlantisresourcesltd.com/turbines/ar-series.html>. ([Online; accessed 19-September-2018])
- Aubry J., Ben Ahmed H., Multon B. (2012). Sizing optimization methodology of a surface permanent magnet machine-converter system over a torque-speed operating profile: Application to a wave energy converter. *IEEE Transactions on Industrial Electronics*, Vol. 59, No. 10, pp. 2116–2125.
- Benelghali S., Benbouzid M. E. H., Charpentier J. F. (2012). Generator systems for marine current turbine applications: A comparative study. *IEEE Journal of Oceanic Engineering*, Vol. 37, No. 3, pp. 123-138.
- Benelghali S. E., Benbouzid M. E. H., Charpentier J. F. (2007). Marine tidal current electric power generation technology: State of the art and current status. In *2007 ieee international electric machines & drives conference*, p. 1407-1412. Antalya, Turkey.
- Campbell R., Martinez A., Letetrel C., Rio A. (2017). Methodology for estimating the french tidal current energy resource. *International Journal of Marine Energy*, Vol. 19, No. Supplement C, pp. 256 - 271.

- Chen H., Ait-Ahmed N., Machmoum M., Zaim M.-H. (2016). Modeling and vector control of marine current energy conversion system based on doubly salient permanentmagnet generator. *IEEE Transactions Sustainable Energy*, Vol. 7, No. 1, pp. 409-418.
- Dieng A., Benkhoris M. F., Claire J. C. L. (2014). Fault-tolerant control of 5-phase pmsg for marine current turbine applications based on fractional controller. In *International federation of automatic control*.
- Fox C. J., Benjamins S., Masden E. A., Miller R. (2017). Challenges and opportunities in monitoring the impacts of tidal-stream energy devices on marine vertebrates. *Renewable and Sustainable Energy Reviews*.
- Grauers A. (1996). *Design of direct-driven permanent-magnet generators*. Phd dissertation, Chalmers University.
- Li H., Chen Z. (2008). Overview of different wind generator systems and their comparisons. In *Renewable Power Generation, IET*, Vol. 2, No. 2, pp. 123-138.
- Mcdonald A. S., Mueller M. A., Polinder H. (2008, March). Structural mass in direct-drive permanent magnet electrical generators. *IET Renewable Power Generation*, Vol. 2, No. 1, pp. 3-15.
- MCT.Ltd. (2012). <http://www.marineturbiness.com>. ([Online; accessed 19-September-2018])
- Mehrzed D., Luque J., Cuenca M. C. (2009). *Vector control of pmsg for wind turbine applications*. Technical report, Aalborg University.
- Openhydro. (2014). <http://www.openhydro.com/home.html>. ([Online; accessed 19-September-2018])
- Panda R. C. (2012). *Introduction to PID controllers-Theory, tuning and application to frontier areas*. InTech.
- Pyrhönen J., Jokinen T., Hrabovcová V. (2014). *Design of rotating electrical machines*. John Wiley & Sons.
- Rourke F., Boyle F., Reynolds A. (2010). Marine current energy devices: Current status and possible future applications in ireland. *Renewable and Sustainable Energy Reviews*, Vol. 14, No. 3, pp. 1026-1036.
- Zhang J. (2015). *Optimization design and control strategies of a double stator permanent magnet generator for tidal current energy application*. Phd dissertation, Université de Nantes.
- Zhang J., Houari A., Seck A., Moreau L., Machmoum M. (2016, March). Fault tolerant control of a double stator permanent magnet generator in tidal current energy system. In *2016 ieee international conference on industrial technology (icit)*, p. 419-424.

